On the white dwarf cooling sequence of the globular cluster ω Centauri[1]

A. Calamida[2,3], C. E. Corsi[2], G. Bono[2,4], P. B. Stetson[5], P. Prada Moroni[6,7], S. Degl'Innocenti[6,7], I. Ferraro[2], G. Iannicola[2], D. Koester[8], L. Pulone[2], M. Monelli[9], P. Amico[4], R. Buonanno[3], F. Caputo[2], S. D'Odorico[4], L. M. Freyhammer[10], E. Marchetti[4], M. Nonino[11], and M. Romaniello[4]

drafted February 2, 2008 / Received / Accepted

ABSTRACT

We present deep and precise photometry ($F435W$, $F625W$, $F658N$) of ω Cen collected with the Advanced Camera for Surveys (ACS) on board the Hubble Space Telescope (HST). We have identified $\approx$ 6,500 white dwarf (WD) candidates, and the ratio of WD and Main Sequence (MS) star counts is found

[1]Based on observations collected with the Advanced Camera for Surveys on board of the Hubble Space Telescope.

[2]INAF-Osservatorio Astronomico di Roma, via Frascati 33, Monte Porzio Catone, Rome, Italy; calamida@mporzio.astro.it

[3]Università di Roma Tor Vergata, via della Ricerca Scientifica 1, 00133 Rome, Italy; buonanno@roma2.infn.it

[4]European Southern Observatory, Karl-Schwarzschild-Str. 2, D-85748 Garching bei Munchen, Germany; pamico@eso.org, sdodoric@eso.org, emarchet@eso.org, mromanie@eso.org

[5]Dominion Astrophysical Obs., HIA, NRC, 5071 West Saanich Road, Victoria BC V9E 2E7, Canada; peter.stetson@nrc-cnrc.gc.ca

[6]Dipartimento di Fisica "E. Fermi", Univ. Pisa, Largo B. Pontecorvo 2, 56127 Pisa Italy; prada@df.unipi.it, scilla@df.unipi.it

[7]INFN, Sez. Pisa, via Largo B. Pontecorvo 2, 56127 Pisa, Italy

[8]Institut fr Theoretische Physik und Astrophysik, University of Kiel, 24098 Kiel, Germany; koester@astrophysik.uni-kiel.de

[9]IAC - Instituto de Astrofisica de Canarias, Calle Via Lactea, E38200 La Laguna, Tenerife, Spain; monelli@iac.es

[10]Centre for Astrophysics, University of Central Lancashire, Preston PR1 2HE; lmfreyhammer@uclan.ac.uk

[11]INAF-Osservatorio Astronomico di Trieste, via G.B. Tiepolo 11, 40131 Trieste, Italy; nonino@oats.inaf.it

to be at least a factor of two larger than the ratio of CO-core WD cooling and MS lifetimes. This discrepancy is not explained by the possible occurrence of a He-enhanced stellar population, since the MS lifetime changes by only 15% when changing from a canonical (Y=0.25) to a He-enhanced composition (Y=0.42). The presence of some He-core WDs seems able to explain the observed star counts. The fraction of He WDs required ranges from 10% to 80% depending on their mean mass and it is at least five times larger than for field WDs. The comparison in the Color Magnitude Diagram between theory and observations also supports the presence of He WDs. Empirical evidence indicates that He WDs have been detected in stellar systems hosting a large sample of extreme horizontal branch stars, thus suggesting that a fraction of red giants might avoid the He-core flash.

Subject headings: globular clusters: general — globular clusters: ω Centauri

1. Introduction

White Dwarfs (WDs) in Galactic Globular clusters (GGCs) represent the intersection of several theoretical and empirical astrophysical problems (Koester 2002; Hansen & Liebert 2003; Hansen 2004). They play a crucial role in constraining the correctness of the physical assumptions adopted to construct WD evolutionary models (Prada Moroni & Straniero 2007). Cluster WDs possess several advantageous features. *Homogeneous sample* – Cluster WDs are located at the same distance and generally have about the same reddening. Moreover, at all luminosities the colors of cluster WDs are systematically bluer than Main Sequence (MS) stars. This means that to properly identify cluster WDs we can use a Color Magnitude Diagram (CMD) instead of a color-color diagram. Therefore, cluster WDs are not affected by the color degeneracy with MS stars that affects field WDs (Hansen & Liebert 2003). *Statistics* – Evolutionary predictions indicate that in a GC with an age of 12 Gyr and a Salpeter-like initial mass function the number of WDs should be three orders of magnitude larger than the number of Horizontal Branch (HB) stars (Brocato et al. 1999). This together with the high stellar concentration implies that the expected density of WDs in GCs is several orders of magnitude larger than in the Galactic field. *Origin* – For cluster WDs we can trace back the evolutionary properties of the progenitors, since both the cluster age and the chemical composition are well known (Kalirai et al. 2007, KA07).

However, cluster WDs also present a few drawbacks. *Crowding* – they are faint objects severely affected by crowding problems (Moehler et al. 2004). *Cluster vs Field* – Current data do not allow us to establish definitively whether cluster WDs are the analogs of field

WDs. The impact that the high density environment of GCs may have on the formation and evolution of cluster WDs is still poorly known (Monelli et al. 2005, MO05).

In a previous investigation based on three out of nine ACS pointings we have already addressed the properties of WDs in ω Cen (MO05). In the meantime, deep photometric investigations called attention to the occurrence of a split along the MS of ω Cen (Bedin et al. 2004). Spectroscopic data have indicated that the stars distributed along the bluer MS (30% of the entire population) are ≈ 0.3 dex more metal-rich than the typical population and probably also He-enriched (Y~ 0.42, Piotto et al. 2005).

2. Observations and data reduction

We use archival multiband ($F435W$, $F625W$, $F658N$) photometric data collected with the ACS on board the HST. The current data set includes eight out of the nine pointings located across the cluster center that have already been discussed by Castellani et al. (2007, see their Fig. 1, CA07). The central pointing of the 3×3 mosaic was omitted due to the severe crowding of the innermost regions. For each field, the $F435W$- and $F625W$-band data consist of one shallow (8s) and three deep (340s each) exposures, while the $F658N$-band data consist of four exposures of 440s each. The raw frames were pre-reduced by the standard HST pipeline. The entire set of images was reduced simultaneously with `DAOPHOT IV/ALLFRAME` and the final catalog includes more than one million stars. The photometry was kept in the Vega system (Sirianni et al. 2005).

Fig. 1 (left) shows the $F435W$, $F435W - F625W$ CMD for selected cluster stars. From this catalog we selected all the stars systematically bluer than MS stars and fainter than extreme HB (EHB) stars ($B \lesssim 20$, see solid black lines in the left panel of Fig. 1). We ended up with a sample of $\approx 60,000$ stars. The photometry of these stars was performed once again using `ROMAFOT`, but only for the deep exposures. Individual stars have been interactively checked in every image, and the WD candidates were measured either as isolated stars or together with neighbor stars. A significant fraction of the originally selected detections turned out to be either cosmic rays or spurious detections close to saturated stars, or detections too faint to be reliably measured on individual images. Fig. 1 also shows the $F435W$, $F435W - F625W$ (middle) and the $F435W$, $F435W - F658N$ (right) CMDs based, this time, on the `ROMAFOT` photometry. Data plotted in these panels show that the candidate cluster WDs ($\sim 6,500$) are distributed along a well defined star sequence fainter than EHB stars and bluer than MS stars (MO05). To our knowledge this is the largest sample of cluster WD candidates ever detected. The current sample is $\approx 40\%$ of the WDs identified in all GGCs combined (Hansen et al. 2004,2007) and $\approx 50\%$ of all spectroscopically confirmed field

WDs (Eisenstein et al. 2006).

3. Results and final remarks

In order to compare theory and observation we have adopted the cooling sequences for CO-core and H-rich envelopes (DA WDs) by Althaus & Benvenuto (1998), for CO-core and He-rich envelopes (DB WDs) by Benvenuto & Althaus,(1997), and for He-core (He WDs) by Serenelli et al. (2002). The theoretical predictions were transformed into the observational plane by adopting the pure H and pure He WD atmosphere models computed by Koester et al. (2005). Predicted magnitudes in the Vega system were computed using the ACS bandpasses (`ftp://ftp.stsci.edu/cdbs/cdbs1/comp/acs`), while their zero-points are based on the Vega spectrum (Bohlin & Gilliland 2004, `ftp://ftp.stsci.edu/cdbs/cdbs2/calspec/`). Fig. 2 shows the comparison, in the $F435W, F435W - F625W$ CMD, between the candidate cluster WDs and predicted cooling sequences for DA (top, CO-core + H envelope), DB (middle, CO-core + He envelope), and He (bottom, He-core) WDs. Note that in this figure we have plotted only stars with $\sigma(F435W - F625W) \leq 0.3$, i.e., objects above a 5-σ detection threshold. Predicted cooling sequences were plotted for a true ω Cen distance modulus $\mu_0 = 13.70 \pm 0.06$ (Del Principe et al. 2006) and a reddening $E(B-V) = 0.11 \pm 0.02$ (Calamida et al. 2005). Using the reddening law from Cardelli et al. (1989) and $R_V = 3.1$, we find $A_{F435W} = 0.46$, $E(F435W - F625W) = 0.17$, and $E(F435W - F658N) = 0.18$. Data plotted in this figure further strengthen the preliminary evidence brought forward by MO05 based on a smaller WD sample: DA and DB WD cooling sequences are, at fixed magnitude, systematically bluer (hotter) than the bulk of candidate cluster WDs. On the other hand, the predicted He WD cooling sequences are consistent with a substantial fraction of the observed candidate WDs. The discrepancy between predicted DA/DB WDs and observations can hardly be caused by the adopted WD atmosphere models. The difference in color at fixed magnitude between the same cooling sequences transformed using WD models provided by Bergeron, Wesemael, & Beauchamp (1995) and our WD models is, for $T_{eff} \geq 10,000$, at most ~ 0.02 mag[12].

To further constrain this circumstantial empirical evidence, MO05 compared the ratio between observed WD and HB star counts with the corresponding evolutionary times. However, CA07 found an apparent excess of HB stars in ω Cen based on a photometric data set covering almost the entire cluster. In order to avoid deceptive uncertainties in the ob-

[12]The $F625W$- and $F658N$-band WD cooling sequences plotted in Figs. 3,4 of MO5 were unknowingly interchanged. This mismatch does not affect the conclusions of that investigation.

served ratios we therefore decided to use MS stars located across the turnoff (TO) region as our reference sample, rather than HB stars. Specifically, we employ the magnitude bin $18.775 \leq B \leq 19.025$ mag (see the green box in Fig. 1) because theory and observations suggest that its population depends minimally on the initial mass function (Zoccali & Piotto 2000) since these stars represent a very small range of mass (CA07). Moreover, this magnitude range is minimally affected by completeness problems. The MS star counts are based on the `ALLFRAME` catalog, while the WD star counts are based on the `ROMAFOT` catalog. The former data set is complete along the MS, while the latter is less contaminated by spurious detections in the WD region. The WDs were selected in three different magnitude bins: $B \leq 24$, 24.5, and 25 (purple, cyan, and red dots in the middle and right panels of Fig. 1) to trace the sample completeness when considering fainter magnitudes. We did not apply any selection criteria to estimate the star counts, apart from the magnitude limits. We found that the observed ratios in the two different CMDs (see lines 1, 2 in Table 1) agree quite well in the brighter magnitude bin (0.052 ± 0.002 vs 0.050 ± 0.002) while they steady decrease in the diagram based upon the narrow $F658N$ bandpass when moving toward fainter magnitudes (0.163 ± 0.004 vs 0.147 ± 0.004). This effect is due to the difference in the completeness between the wide $F625W$ and the narrow $F658N$ band, the latter obviously being shallower. In order to constrain the dependence on the adopted MS sample, we counted MS stars once again in the box $19.025 \leq B \leq 19.275$ mag. Ratios listed in Table 1 show that the difference in the brighter bin is on average $\approx 16\%$.

In order to define the typical stellar mass of MS turn-off stars we adopted two cluster isochrones for $t = 12$ Gyr (see top panel in Fig. 2) with canonical primordial helium content Y=0.25 (Spergel et al. 2007) and metal abundances (Z=0.0004, Z=0.0015) that bracket the observed spread in metallicity of ω Cen stars (Sollima et al. 2005; Villanova et al. 2007). These isochrones were transformed into the observational plane using the atmosphere models provided by Brott & Hauschildt (2005). The above isochrones are based on evolutionary tracks computed with an updated version of the FRANEC evolutionary code (Chieffi & Straniero 1989) including microscopic element diffusion (Cariulo et al. 2004; CA07). In order to estimate the lifetime spent by MS stars in crossing the specified magnitude bin we constructed two evolutionary tracks with $M/M_{\odot}$=0.75 (Z=0.0004) and $M/M_{\odot}$=0.78 (Z=0.0015). We found that the average crossing time for these two tracks is ≈ 950 Myr. The predicted lifetime ratios between DA/DB WD (M_{WD}=0.5-0.9 $M_{\odot}$) and MS (M_{MS}=0.75-0.78 $M_{\odot}$) stars attain, within the uncertainties, quite similar values (see lines 3 to 6 in Table 1). The errors in the lifetime ratios include an uncertainty of $\approx 10\%$ in the adopted input physics (CA07). The ratios for He WDs are, as expected, larger and in the brighter bin ($F435W \leq 24$) they are at least a factor of three larger than CO-core ratios (see lines 7 to 9 in Table 1). To estimate possible uncertainties in distance and in the reddening correction,

we adopted a larger apparent distance modulus (DM_B=14.36 vs 14.16). The difference in the two sets of lifetime ratios for M_{WD}=0.5 is at most 18%.

This comparison between theory and observation indicates that the star count ratios in the brighter magnitude bin (see Fig. 3) are at least a factor of two larger than predicted by DA/DB WD cooling times. On the other hand, the observed ratios are at least a factor of four smaller than predicted by He WD cooling times. The discrepancy between the observed WD star counts and the predicted CO-core ratios can hardly be explained by incompleteness problems affecting the sample of candidate WDs, which would go in the direction of increasing the discrepancy between theory and observation. The same conclusion would apply for a putative increase in the mean mass of CO-core WDs, since the lifetime ratios on average decrease—as expected—by at least a factor of two (see lines 4, 6 in Table 1). An increase in the mean mass of He WDs, on the other hand, does not imply a steady decrease in the cooling lifetime (see lines 7 to 9 in Table 1). This nonlinear behavior is due to the occurrence of CNO thermonuclear flashes in the mass range $0.22 \lesssim M/M_{\odot} \lesssim 0.422$ (Serenelli et al. 2002). The lifetime ratios quoted above indicate that predicted He WD lifetimes are at least a factor of two larger than observed.

The quoted discrepancies are also minimally affected by a decrease in the cluster age of 2 Gyr (see middle panel of Fig. 2). We constructed two evolutionary tracks with $M/M_{\odot} = 0.77$ (Z=0.0004) and $M/M_{\odot} = 0.80$ (Z=0.0015) and found that the mean time they spend in crossing the specified magnitude bin is only 10% shorter than for the older models (see lines 10 to 14 in Table 1). Therefore, this decrease in the assumed age hardly affects the discrepancy between theory and observations. As another attempt to account for our findings we also considered a possible increase in the He content of MS stars. In particular, we adopted two cluster isochrones with same age and metal abundances as the canonical ones, but with a He-enhanced ($Y = 0.42$) composition (see bottom panel of Fig. 2). In order to represent a possible spread in He content, we estimated the predicted ratios for a mix of stellar populations consisting of 70% stars with canonical He content (Y=0.25) and 30% He-enhanced stars. We constructed two He-enhanced evolutionary tracks with $M/M_{\odot}$=0.55 (Z=0.0004) and $M/M_{\odot}$=0.57 (Z=0.0015) and found that the mean lifetime they spend in the specified magnitude bin is 460 Myr. Therefore, the MS lifetimes of the mixed-He population decrease by only $\sim$ 15% (800 vs 950 Myr) relative to the canonical population. Data plotted in Fig. 3 (see also Table 1) indicate that the occurrence of a He-enhanced sub-population in ω Cen can not by itself explain the discrepancy between the star counts and the lifetime ratios.

Let us assume, as a working hypothesis, that the current sample of candidate cluster WDs represents a mix of CO-core and He-core WDs. The aforementioned lifetimes suggest

that the fraction of He WDs ranges from 80% (if we assume a mean mass of $0.5M_{\odot}$ for the CO-core and $0.3M_{\odot}$ for the He-core WDs) to 10% (for a mean mass of $0.5M_{\odot}$ for the CO-core and $0.23M_{\odot}$ for the He-core WDs). The latter fraction decreases further if we assume still smaller He-core WDs, but current empirical estimates indicate that the lower limit ranges from $\approx$ 0.17 to $\approx$ 0.2 $M_{\odot}$ (Moehler et al. 2004; Kepler et al. 2007). This evidence, if supported by independent spectroscopic measurements, indicates that cluster WD samples might present different intrinsic properties when compared with field WDs. Current estimates based on the large SDSS sample of WDs indicate that only 2% of field DA WDs possess masses smaller than $0.45M_{\odot}$. Note that the current fraction of He-core WDs is different by only a factor of 2-3 from the global binary frequency in ω Cen (Mayor 1996) and in good agreement with the binary fraction ($\approx$ 10%) in GCs in general (Davies et al. 2006). A similar excess of He WDs in the old open cluster NGC 6791 was proposed by KA07. They found that roughly 40% of the WDs in this system did not experience the expected core-helium flash at the tip of the red giant branch (RGB). These objects end their evolution as He-core WDs after having lost a significant fraction of their envelope. According to evolutionary prescriptions they are the aftermath of an extreme mass loss episode possibly caused either by stellar collisions or by close binary interactions (Castellani et al. 2006a,b, CA06a, CA06b). However, Bedin et al. (2005), using deep ACS images, suggested that the color distribution of WDs in NGC 6791 does not support the occurrence of He WDs.

The available observations present, as suggested by the referee, puzzling empirical aspects. Detailed photometric investigation of WDs in GCs like M4 (Hansen et al. 2004) and NGC 6397 (Hansen et al. 2007) do not show evidence for He-core WDs. On the other hand, Sandquist & Martel (2007) found a well defined deficiency ($\approx$ 20%) of bright RGs in NGC 2808 and suggested that the missing giants might produce He-core WDs. An enhanced mass loss efficiency, driven by metal content, was suggested by KA07 to account for He-core WDs in NGC 6791. However, the peak in the metallicity distribution of ω Cen (Kayser et al. 2006) and the metallicity of NGC 2808 (Carretta 2006) are at least 1.5 dex more metal-poor than NGC 6791. A possible He enrichment has been proposed to account for EHB stars and the complex MS structure in ω Cen and in NGC 2808 (D'Antona et al. 2002; Piotto et al. 2007). If we assume a canonical helium-to-metal enrichment ratio ($\Delta Y/\Delta Z \approx 2.5$) a similar enhancement could also be present in NGC 6791. However, WD/MS and HB/MS (CA07) star count ratios in ω Cen do not seem to support this hypothesis: for a canonical enrichment ratio, the putative He-rich stars in ω Cen should have above Solar metallicities. A single simple hypothesis of stellar evolution driven by cluster structural parameters and dynamical evolution can hardly account for the quoted He WD identifications, since the central density in ω Cen and in NGC 2808 is significantly larger than in NGC 6791. Therefore, we are left with compelling evidence that He WDs have been detected/predicted in

stellar systems that host sizable samples of EHB stars (ω Cen, CA07; NGC 2808, CA06a; NGC6791, KA07). However, the natural progeny of EHB stars are CO-core WDs. The He enrichment scenario can account for EHB stars, but does not explain, for canonical mass loss rates, the occurrence of He WDs. On the other hand, if a substantial fraction of RGs avoids the He-core flash, they will end up their evolution, according to the residual envelope mass, either as EHB/CO-core WDs or as He-core WDs (Hansen 2005; CA06b).

REFERENCES

Althaus, L. G., & Benvenuto, O. G. 1998, MNRAS, 296, 206

Bedin, L. R., et al. 2004, ApJ, 605, L125

Bedin, L. R., et al. 2005, ApJ, 624, L45

Benvenuto, O. G., & Althaus L. G. 1997, MNRAS, 288, 1004

Bergeron, P., Wesemael, F., Beauchamp, A. 1995, PASP, 107, 1047

Bohlin, R. C., & Gilliland, R. L. 2004, ApJ, 127, 3508

Brocato, E., Castellani, V., & Romaniello, M. 1999, A&A, 345, 499

Brott, I., Hauschildt, P. H. 2005, in The 3-D Universe with Gaia, ed. C. Turon, K. O'Flaherty & M. Perryman, ESA SP-576, 565

Calamida, A., et al. 2005, ApJ, 634, L69

Cardelli, J. A., Clayton, G. C., Mathis, J.S. 1989, ApJ, 345, 245

Cariulo, P., Degl'Innocenti S., Castellani, V. 2004, A&A 421, 1121

Carretta, E. 2006, AJ, 131, 1766

Castellani, M., Castellani, V., Prada Moroni, P. 2006, A&A, 457, 569 (CA06a)

Castellani, V., et al. 2006, A&A, 446, 569 (CA06b)

Castellani, V., et al. 2007, ApJ, 663, 1021 (CA07)

Chieffi, A., & Straniero, O. 1989, ApJS, 71, 47

Davies, M. B., et al. 2006, NewA, 12, 201

D'Antona, F. et al. 2002, A&A, 395, 69

Del Principe, M. et al. 2006, ApJ, 652, 362

Eisenstein, D. J., et al. 2006, ApJS, 167, 40

Hansen, B. M. S. 2004, PhR, 399, 1

Hansen, B. M. S. 2005, ApJ, 635, 522

Hansen, B. M. S., & Liebert, J. 2003, ARA&A, 41, 465

Hansen, B. M. S., et al. 2004, ApJS, 155, 551

Hansen, B. M. S., et al. 2007, astro-ph/0701738

Kalirai, J. S., et al. 2007, astro-ph/07050977v2 (KA07)

Kayser, A., et al. 2006, A&A, 458, 777

Kepler, S. O., et al. 2007, MNRAS, 375, 1315

Koester, D. 2002, A&ARv, 11, 33

Koester, D., et al. 2005, A&A, 439, 317

Mayor, M., ASPC, 90, 190

Moehler, S. et al. 2004, A&A, 420, 515

Monelli, M., et al. 2005, ApJ, 621, L117 (MO05)

Piotto, G., et al. 2005, ApJ, 621, 777

Piotto, G., et al. 2007, ApJ,661, L53

Prada Moroni, P. & Straniero, O. 2007, A&A, 466, 1043

Sandquist, E. L, & Martel, A. R. 2007, ApJ, 654, L65

Serenelli A. M., Althaus L. G., Rohrmann R. D., & Benvenuto, O. G. 2002, MNRAS, 337, 1091

Sirianni, M., et al. 2005, PASP, 117, 1049

Sollima, A. et al. 2005, ApJ, 634, 332

Spergel, D. N., & WMAP collaboration 2007, ApJS, 170, 377

Villanova, S., et al. 2007, ApJ, 663, 296

Zoccali, M.,& Piotto, G. 2000, A&A, 358, 943

Table 1. Ratios between CO and He WD cooling times and MS lifetimes

$F435W$	24.0		24.5		25.0	
N_{WD}/N_{MS}	0.052(2)[a]	0.044(2)[b]	0.095(2)[a]	0.080(2)[b]	0.163(4)[a]	0.137(3)[b]
N_{WD}/N_{MS}	0.050(2)[c]	0.042(2)[d]	0.090(3)[c]	0.076(3)[d]	0.147(4)[c]	0.124(3)[d]
DA[0.5][e]	0.021(3)[f]	0.019(2)[g]	0.048(7)[f]	0.044(6)[g]	0.12(2)[f]	0.11(2)[g]
DA[0.9][e]	0.0045(6)[f]	0.0029(4)[g]	0.029(4)[f]	0.018(2)[g]	0.08(1)[f]	0.08(1)[g]
DB[0.5][e]	0.021(3)[f]	0.020(2)[g]	0.057(8)[f]	0.047(7)[g]	0.13(2)[f]	0.13(2)[g]
DB[0.9][e]	0.0040(5)[f]	0.0034(5)[g]	0.016(2)[f]	0.008(1)[g]	0.07(1)[f]	0.050(7)[g]
He[0.23][e]	0.35(5)[f]	0.38(5)[g]	0.51(7)[f]	0.57(8)[g]	0.70(10)[f]	0.80(11)[g]
He[0.3][e]	0.07(1)[f]	0.040(6)[g]	0.18(3)[f]	0.17(2)[g]	0.33(5)[f]	0.34(5)[g]
He[0.45][e]	0.15(2)[f]	0.15(2)[g]	0.32(4)[f]	0.30(4)[g]	0.63(9)[f]	0.61(9)[g]
DA[0.5][e]	0.019(3)[h]	0.024(3)[i]	0.044(6)[h]	0.057(8)[i]	0.11(2)[h]	0.14(2)[i]
DB[0.5][e]	0.019(3)[h]	0.024(3)[i]	0.052(7)[h]	0.067(9)[i]	0.12(2)[h]	0.16(2)[i]
He[0.23][e]	0.32(5)[h]	0.42(6)[i]	0.47(7)[h]	0.61(8)[i]	0.64(9)[h]	0.82(2)[i]
He[0.3][e]	0.07(1)[h]	0.08(1)[i]	0.17(2)[h]	0.21(3)[i]	0.30(4)[h]	0.39(5)[i]
He[0.45][e]	0.14(2)[h]	0.18(3)[i]	0.29(4)[h]	0.37(5)[i]	0.58(8)[h]	0.75(11)[i]

[a]Star counts based on the $F435W, F435W - F625W$ CMD and the MS box at $B = 18.90$. Numbers in parentheses are the uncertainties on the last decimal figures(s).

[b]Star counts based on the $F435W, F435W - F625W$ CMD and the MS box at $B = 19.15$.

[c]Star counts based on the $F435W, F435W - F658N$ CMD and the MS box at $B = 18.90$.

[d]Star counts based on the $F435W, F435W - F658N$ CMD and the MS box at $B = 19.15$.

[e]Predicted cooling and lifetime ratios for CO-core (DA,DB) and He-core WDs. Numbers in square brackets are the WD masses in solar units.

[f]Estimates based on a distance modulus of $DM_B = 14.16$.

[g]Estimates based on a distance modulus of $DM_B = 14.36$.

[h]Estimates based on a cluster age of 10 Gyr.

[i]Estimates based on 70% He-normal (Y=0.25) and 30% He-enriched (Y=0.42) stars.

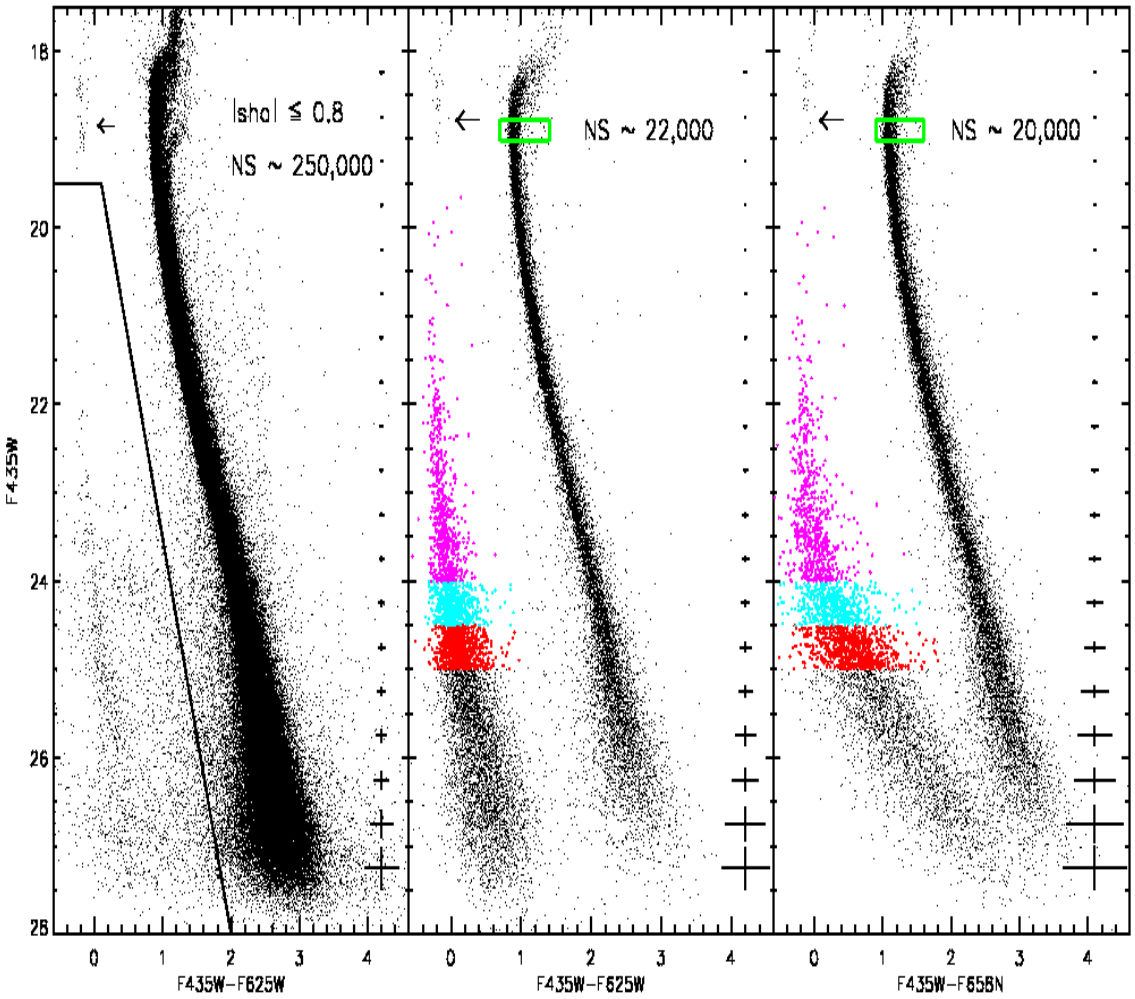

Fig. 1.— Left – F435W, F435W-F625W CMD based on data collected with ACS@HST and reduced with `ALLFRAME`. Stars plotted in this diagram were selected according to *sharpness* and *separation*. The solid black lines show magnitude and color ranges of the candidate cluster WDs. The arrow marks EHB stars, while the error bars on the right display intrinsic errors in magnitude and color. Middle – F435W, F435W-F625W CMD based on deep images collected with ACS@HST and reduced with `ROMAFOT`. The MS and the TO regions are less populated because only the stars located close to candidate WDs have been measured. Moreover, stars with $F435W \lesssim 18$ are saturated in deep images. The green box shows TO region adopted for MS star counts. Candidate WDs with $F435W \leq 24$, 24.5, and 25 are marked with different colors. Right – Same as the middle, but for the F435W, F435W-F658N CMD.

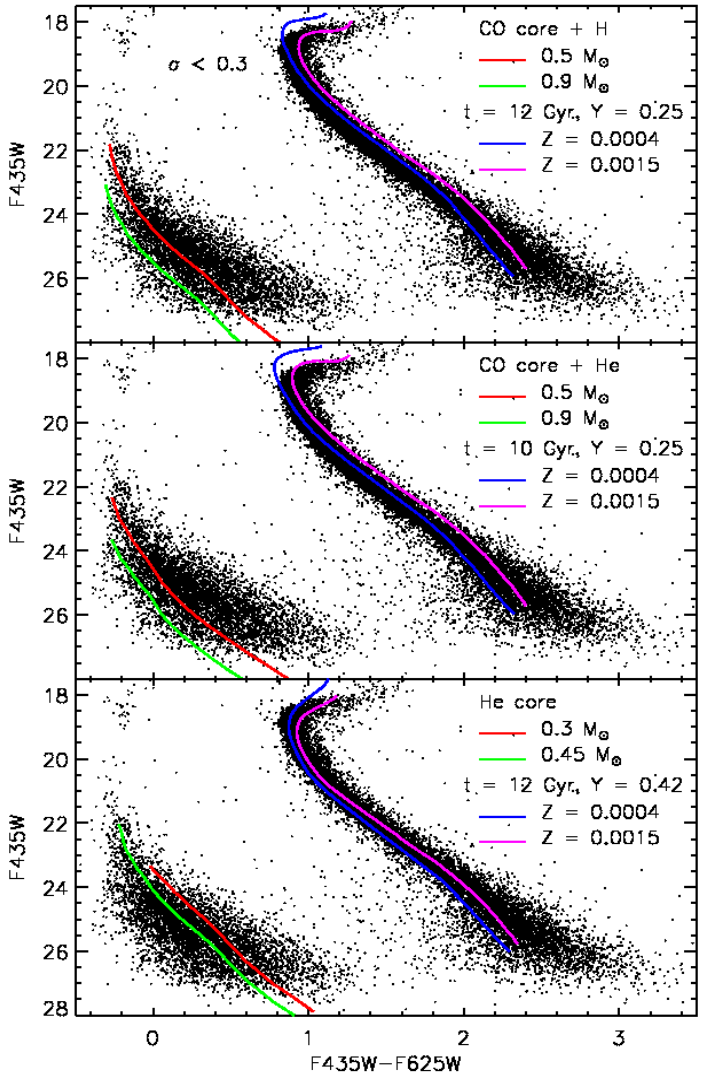

Fig. 2.— Top – F435W, F435W-F625W CMD, only stars with $\sigma(F435W - F625W) \leq 0.3$ are plotted. The green and the red line show the cooling sequences for selected DA (CO-core + H envelope) WDs, while the blue and the purple line are two cluster isochrones for $t = 12$ Gyr and different metal abundances (see labeled values). Middle – same as the top, but the cooling sequences refer to DB (CO-core + He envelope) WDs and two isochrones for $t = 10$ Gyr. Bottom – same as the top, but the cooling sequences refer to He-core WDs and two isochrones for $t = 12$ Gyr and a He-enhanced (Y=0.42) chemical composition.

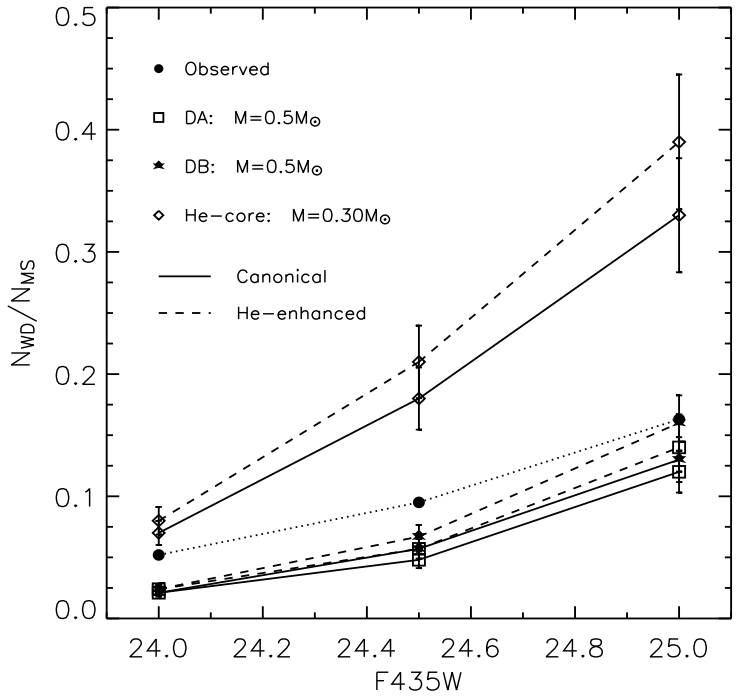

Fig. 3.— Star count ratios (N_{WD}/N_{MS}) and predicted ratios between WD cooling times and MS lifetimes versus $F435W$ magnitude. Solid and dashed lines show the ratios for He-normal and He-enhanced structures.